CHALMERS

Sensor data fusion for road friction estimation

Master of Science Thesis in Systems, Control & Mechatronics

JOHAN BÖRGESON
ANTON STÅLHEIM

Department of Signals and Systems
Division of Signal Processing
CHALMERS UNIVERSITY OF TECHNOLOGY
Göteborg, Sweden 2010

Master of Science Thesis EX053/2010

MASTER OF SCIENCE THESIS EX053/2010

Sensor data fusion
for road friction estimation

Master of Science Thesis in Systems, Control & Mechatronics

JOHAN BÖRGESON
ANTON STÅLHEIM

Department of Signals and Systems
Division of Signal Processing
CHALMERS UNIVERSITY OF TECHNOLOGY

Göteborg, Sweden 2010

Sensor data fusion
for road friction estimation
JOHAN BÖRGESON
ANTON STÅLHEIM

Master of Science Thesis EX053/2010
Department of Signals and Systems
Division of Signal Processing
Chalmers University of Technology
SE-412 96 Göteborg
Sweden
Telephone: + 46 (0)31-772 1000

Cover:
Slippery road traffic warning sign

Chalmers Reproservice
Göteborg, Sweden 2010

Sensor data fusion
for road friction estimation
Master of Science Thesis in Systems, Control & Mechatronics
JOHAN BÖRGESON
ANTON STÅLHEIM
Department of Signals and Systems
Division of Signal Processing
Chalmers University of Technology

Abstract

In vehicle dynamics, tire-to-road friction is the most important factor for force-transfer between vehicle and road. Without friction the vehicle would not be able to move at all. The variation of tire-to-road friction can be large, and can reach dangerously low levels. It is therefore of great value to be able to estimate available tire-to-road friction. Lot of effort has been spent on research in the area for many years and the increasing number of sensors opens up for new possibilities in friction estimation.

This thesis presents a robust sensor fusion method for tire-to-road friction estimation able to handle several information sources. A Bayesian approach that uses information from stability systems and road surface classification information is proposed. The method uses a Kalman filter with a forgetting function modification. This approach allows the distribution to converge to a predefined *a priori* distribution according to present road surface. The method is used to investigate the possibilities with road surface information sensors.

Simulations and tests have been run to verify and evaluate the performance and behavior of the filter. Several performance parameters are defined that allows a fair comparison of different input data.

Results show that the fusion algorithm works as intended and takes different information sources into account when calculating the estimate and uncertainty. The road surface classification shows good potential of improving both availability and correctness of the friction estimate. This is due to the road surface being the most important parameter in tire-to-road friction, using this information result in low estimation bias.

Keywords: road friction estimation, sensor fusion, tire friction estimation

Preface

In this study the use and possibilities with sensor fusion for road friction estimation have been analyzed. Previous work concerning friction estimation from vehicle dynamic sensors has been merged with information from new sensors able to classify road surface conditions. The work has been carried out at Volvo Car Corporation, Driver Support group, from February 2010 until July 2010. The thesis has been written by students Johan Börgeson and Anton Stålheim. Supervisors at Volvo Car Corporation have been Johan Rönnberg, Joakim Lin-Sörstedt and Lars Danielsson. Lennart Svensson has been supervisor and examiner at Signals and Systems at Chalmers University of Technology.

Aknowledgements

We would like to thank our primary supervisor Johan Rönnberg at Volvo Car Corporation for his industrious help during the project. We would also thank his fellow co-workers, and also our supervisors, Joakim Lin-Sörstedt and Lars Danielsson for their valuable feedback concerning sensor fusion. At the Department of Signals and Systems Lennart Svensson our supervisor/examiner has given us support and helped us keeping the project on track. Erik Bergvall at Volvo Car Corporation has given us much help with simulations in VCTS (Volvo Cars Traffic Simulator) and does therefore earn special thanks.

Göteborg August 2010
Johan Börgeson, Anton Stålheim

Contents

List of Figures

List of Tables

Acronyms

- ABS - Anti-Lock Braking System
- DCC - Dynamic Cornering Control
- DSTC - Dynamic Stability and Traction Control
- PDF - Probability Density Function
- RMS - Root Mean Square
- RSC - Road Surface Classification
- TCS - Traction Control System
- VCC - Volvo Car Corporation
- VCTS - Volvo Cars Traffic Simulator

Notations

Subscripts (unless other stated):

- X_f, X_r - Front and rear wheels.
- X_x - Longitudinal direction
- X_y - Lateral direction
- X_k - At time instant k
- X_{k-1} - Value at previous time instant
- X_i - Iterative index

Super scripts:

- X^- - Notation for *a priori*
- $\mathbf{X}^T$ - Matrix transpose
- $\mathbf{X}^{-1}$ - Matrix inverse

Other notations:

- $\mathbf{X}$ - Bold typed variables is notation for vectors.
- $\dot{X}$ - Time derivate of variable X
- $X(t)$ - At time t
- $p(X)$ - The PDF (probability density function) of variable X
- $\sim N(X, Y)$ - Normally distributed with mean X and variance Y
- $\hat{X}$ - Estimation of variable X
- $E[\cdot]$ - Expected value function

- $Cov[\cdot]$ - Covariance for $\cdot$
- $X \in [A, B)$ - X is in interval A-B, A is allowed but not B
- $\lfloor X \rfloor$ - Variable X is *floored* to integer value

Symbols, in order of appereance:

- σ_x - Longitudinal slip ratio
- r_{eff} - Effective rolling radius of tire
- ω_w - Rotational wheel velocity
- V_x - Wheel axle's forward velocity
- $F_{x,f}, F_{x,r}$ - Front and rear wheels longitudinal tire force
- $C_{\sigma,f}, C_{\sigma,r}$ - Front and rear wheels tire stiffness
- α_f, α_r - Side slip angles
- δ - Steering angle
- $\theta_{v,f}, \theta_{v,r}$ - Front and rear wheel's velocity angle in relation to vehicle longitudinal axle.
- V_y - Wheel axle's lateral velocity
- l_f, l_r - Longitudinal distances from the center of gravity to the front and rear wheels
- $\dot{\Psi}$ - Vehicle yaw rate
- $F_{y,l}, F_{y,r}$ - Front and rear wheels lateral tire force
- $\mathbf{x}$ - State vector
- $\mathbf{u}$ - Input vector
- $f(\cdot)$ - Arbitrarily function for process update
- $h(\cdot)$ - Arbitrarily function for measurements/output
- T_s - Sampling interval
- $\mathbf{A}, \mathbf{B}, \mathbf{C}, \mathbf{D}, \mathbf{H}$ - Linear matrices for process (A,B) and measurements (C,D,H)
- $\mathbf{\Phi}, \mathbf{\Gamma}$ - Discrete linear process matrices
- $\mathbf{v}$ - Process disturbances vector
- $\mathbf{w}$ - Measurement disturbances vector
- $\mathbf{z}$ - Measurements vector
- Q - Process noise covariance
- R - Measurement noise covariance

- ε_k - Estimation error, at time instant k
- P_k - Estimation error covariance
- K_k - Kalman gain matrix
- I - Identity matrix
- μ_{max} - Maximum available road friction
- γ - Forgetting function, described in section 4.2
- μ - Statistical mean
- σ^2 - Variance
- $\lambda_{distance}$ - Design parameter, distance before reaching a certain value
- V_{fwd} - Vehicle's forward velocity

1 Introduction

To know whether the road is slippery or not has been of interest since vehicles started driving on the roads. As of today there is no good continuous estimation of the road friction in the vehicles at all times. With stability systems such as the anti-lock braking system (ABS) and traction control system (TCS) a good momentary estimation of the friction can be obtained. This estimation is not valid if the road conditions change. With the increasing number of information sources available in today's cars this project aims at merging direct estimations with information from road surface sensors to a reliable continuous estimate of the road friction. How the performance depends on different information sources will also be investigated and a recommendation of further development will be presented.

The benefit of this improved estimate is e.g. improved performance of active safety systems and active warnings to the driver. In the case of active safety systems it is thus important for the internal system of the car to have information about low friction; even if the driver already knows that it is slippery. In slippery road conditions the accident rate is higher [1], additional information may reduce road accidents.

1.1 Purpose

The purpose of this project is to use information from several sensor sources to merge data into a continuous estimate of the tire-to-road friction coefficient. Using different sensors to eliminate their individual flaws, a more confident and robust tire-to-road friction estimate is achieved.

The focus of this project is to:

- Create a filter framework able to handle arbitrary sensor data, with focus on road surface classification and several direct measurements, to produce an optimal tire-to-road friction estimate.
- Set up a test scenario, define performance measurements to test, tune and evaluate the filter.
- Using information and knowledge gained during the project to specify some future work areas that are of interest.

1.2 Limitations

Due to time limitations all aspects concerning the project will not be performed. The main focus is to develop a filter framework able to handle one indirect information source and several direct measurements. The tire-to-road friction is assumed to be known in these sensors and methods; no time has been spent on further development of individual estimation techniques.

Some physical limitations have also been made. The road surface classification is assumed to be able to distinguish four different surfaces: ice, snow, wet asphalt and dry asphalt. Other conditions such as e.g. extremely hot asphalt, oil spills and aqua-planning is left for future work. In this project the surface is also seen as homogenous close to the vehicle. The probability density function (PDF) for tire-to-road friction, given the four surfaces, is assumed to be known and has not been further investigated.

The project is validated using test results in simulations; one scenario with log data from recorded runs is also used. To get realistic driving behavior in simulations, recorded position and speed profiles is used. This method captures real driving situations, while still having the ability to control the friction. No verifying tests is made in real world experiments.

1.3 Outline

The first section gives an introduction to the subject and why it is important to have information regarding the tire-to-road friction. The main purpose and limitations are also stated here. Next the reader gets some background information about tire mechanics, tire-to-road friction and some filter theory. This is to facilitate further understanding in the report. The input data from stability systems estimate and road surface classification is described in the input data section. It is also explained how sensor input is simulated. This is followed by a description about the algorithm and how it is implemented using a Kalman filter.

In the performance and functionality section measurements for correctness and availability are defined, the simulation and log scenarios are also described. The result section for the simulation model is straightforward and presents the obtained result. Comments, figures and performance measurements on the result are also displayed here. This is followed by the result section for log data which structured in the same way. Discussion and analysis of the results can be found in the discussion section, the focus is on the simulation scenario and the behavior of graphs and performance measurements are explained. Next is a conclusion section that summarizes what conclusions that can be drawn from the results. In the end some further development and improvements are discussed in a future work section.

2 Theory

The objective of this section is to give a brief introduction to some of the underlying theory concerning the tire-to-road friction estimation problem and the proposed filter approach.

2.1 Tire mechanics

This section gives a brief introduction to tire mechanics. The purpose of the tire is, besides make the ride a bit more comfortable, to transfer forces from the vehicle to the road. Without this force-transfer the vehicle would not be able to move.

The tire forces can be divided into longitudinal and lateral forces. It has been shown that the longitudinal forces are a function of longitudinal slip ratio [2]. The longitudinal slip ratio is the difference in longitudinal movement in the outer contact patch and the wheel axle's velocity.
The slip ratio is defined as:

$$\begin{aligned} \sigma_x &= \frac{r_{eff}\omega_w - V_x}{V_x} \quad (braking) \\ \sigma_x &= \frac{r_{eff}\omega_w - V_x}{r_{eff}\omega_w} \quad (acceleration) \end{aligned} \tag{2.1}$$

Where r_{eff} is the effective rolling radius of the tire, ω_w the rotational velocity and V_x the wheel axle's forward velocity.

At small slip ratio ($<$ 10% for dry surfaces) the force is proportional to the slip [2], therefore:

$$\begin{aligned} F_{x,f} &= C_{\sigma,f}\sigma_{x,f} \\ F_{x,r} &= C_{\sigma,r}\sigma_{x,r} \end{aligned} \tag{2.2}$$

Where $C_{(\cdot),(\cdot)}$ are tire stiffness constants.

The maximum longitudinal tire force is mainly reached at 10-15% slip ratio [3]. Further increase in slip ratio results in less tire force why it is desirable to maintain in the 10-15% slip region for full force utilization.

Lateral tire forces are, in the same way as above, due to lateral slip. Lateral slip is often denoted as side-slip angle, it is defined as:

$$\begin{aligned} \alpha_f &= \delta - \theta_{v,f} \\ \alpha_r &= -\theta_{v,r} \end{aligned} \tag{2.3}$$

Where δ is steering angle, $\theta_{v,f}$ & $\theta_{v,r}$ is the front and rear wheel's velocity angle in relation to vehicle longitudinal axle.

Also the lateral force can be approximated to be proportional to slip-angle for small angles [2]. The wheel's velocity angle is defined as:

$$\begin{aligned} tan(\theta_{v,f}) &= \frac{V_y + l_f\dot{\Psi}}{V_x} \\ tan(\theta_{v,r}) &= \frac{V_y - l_r\dot{\Psi}}{V_x} \end{aligned} \tag{2.4}$$

Where V_y is lateral velocity, V_x longitudinal velocity, l_f & l_r is the longitudinal distances from the center of gravity to the front and rear wheels and $\dot{\Psi}$ is the vehicles yaw rate.

With small angles approximation the lateral tire forces can be expressed as in equation 2.5. [2]

$$
\begin{aligned}
F_{y,f} &= C_\alpha(\delta - \frac{V_y + l_f\dot{\Psi}}{V_x}) \\
F_{y,r} &= C_\alpha(-\frac{V_y - l_r\dot{\Psi}}{V_x})
\end{aligned}
\tag{2.5}
$$

2.2 Tire-to-road friction model

In order to calculate, and thereby simulate, tire behavior and forces a mathematical model of the tire is needed. There are several well approved tire models used for this purpose. Only one model will be briefly discussed here.

2.2.1 Brush model

The brush model repose on the tire seen as small elastic bristles. These bristles are stretched lateral in the contact patch and are infinitesimal in longitudinal direction. The model is built with some assumptions. The elasticity of the bristles is assumed to be linearly even though rubber isn't. The carcass of the tire is also assumed to be stiff, which results in the carcass deformation effects to be neglected.

The idea of the model is that the tire force generation can be divided into two regions. In the first region the forces is due to adhesion in the elastic deformation of rubber. In the second region all bristles are assumed to slide, and thus generating sliding friction [4].

2.3 Filter theory

In this section some background on filter theory will be explained. Only the parts of filter theory that are used in our work are presented here. There is rigorous amount of available literature covering this subject and the extent of this section is kept to a minimum. Interested readers are encouraged to consult literature references for deeper knowledge [5, 6, 7, 8].

2.3.1 State-space modeling

When modeling dynamic systems a state-space approach gives good representation of the problem. Information regarding the system can be stored into a state vector. The state-space system is described with two equations. The first equation describes the dynamic relation of the system and how it changes with time and its possible inputs. Second equation defines how outputs/measurements are related to the system [8].

The state-space system can be continuous, discrete or even both. In continuous state-space the process equations notes how the system changes with time (equation 2.6). Discrete state-space equations describe what the state will be the next time instant (equation 2.7). In both cases $\mathbf{x}$ is a vector of all states $x_1, x_2, ..., x_n$ and $\mathbf{u}$ is a vector of possible input signals $u_1, u_2, ..., u_m$

$$\begin{aligned} \dot{\mathbf{x}}(t) &= f(t, \mathbf{x}(t), \mathbf{u}(t)) \\ \mathbf{y}(t) &= h(t, \mathbf{x}(t), \mathbf{u}(t)) \end{aligned} \tag{2.6}$$

$$\begin{aligned} \mathbf{x}_k &= f_{k-1}(\mathbf{x}_{k-1}, \mathbf{u}_{k-1}) \\ \mathbf{y}_k &= h_k(\mathbf{x}_k, \mathbf{u}_k) \end{aligned} \tag{2.7}$$

Both $f(\cdot)$ and $h(\cdot)$ are known, possibly nonlinear functions mapping state and input vectors to next state/change. In the continuous case the states are updated at all time while the discrete state-space only is updated at defined time instants. The time interval is often set as constant T_s but might also be a function of other dependencies.

Whenever one of either f or h functions is nonlinear, the entire system is considered to be nonlinear. When the system is defined as linear, the functions f and h can be expressed as matrices instead. The system can then be noted as equation 2.8 (continuous) or 2.9 (discrete). Note that the matrices still can be time-dependent.

$$\begin{aligned} \dot{\mathbf{x}}(t) &= \mathbf{A}(t)\mathbf{x}(t) + \mathbf{B}(t)\mathbf{u}(t) \\ \mathbf{y}(t) &= \mathbf{C}(t)\mathbf{x}(t) + \mathbf{D}(t)\mathbf{u}(t) \end{aligned} \tag{2.8}$$

$$\begin{aligned} \mathbf{x}_k &= \mathbf{\Phi}_{k-1}\mathbf{x}_{k-1} + \mathbf{\Gamma}_k\mathbf{u}_{k-1} \\ \mathbf{y}_k &= \mathbf{C}_k\mathbf{x}_k + \mathbf{D}_k\mathbf{u}_k \end{aligned} \tag{2.9}$$

Only the discrete cases will be dealt with in this report from here on.

2.3.2 Stochastic and probabilistic system process

The model and state-space system described in previous section assumes an ideal system without any disturbances, neither process disturbances, modeling uncertainties nor measuring noise. Since this is rarely the case in reality, the system model needs to handle these disturbances. One way of dealing with this problem is to model the system as in equation 2.10, where $\mathbf{v}_k$ is process disturbances and model uncertainties and $\mathbf{w}_k$ is measuring noise. The problem is then to find expressions for v and w. By assuming that these disturbances are stochastic variables some important and usable properties is evolved [9].

$$\begin{aligned} \mathbf{x}_k &= f_{k-1}(\mathbf{x}_{k-1}, \mathbf{u}_{k-1}, \mathbf{v}_{k-1}) \\ \mathbf{y}_k &= h_k(\mathbf{x}_k, \mathbf{u}_k, \mathbf{w}_k) \end{aligned} \tag{2.10}$$

Considering the system to be in probabilistic form together with the disturbances being modeled as stochastic variables some important and well-approved methods for dynamic system problems can be used. Given a stochastic process the *Markov property* says that, given information on the present state, the future state does not depend on the past. This makes it only necessary to save information on present states [10].

2.3.3 System estimation

The problem is often to *estimate* the states of a specific system. Properties described in previous sections, the system is e.g. stochastic and probabilistic, makes the use of some well-approved *Bayesian approach* suitable for the problem. Measuring the output from the system, together with some prior dynamic information of the problem, makes it possible to estimate or predict present or future system state [11].

Having information on either present or previous state of the system, one attempts to predict the *a priori* distribution of the system for the next instant. This step uses information on how the system would evolve over one time instant and is calculated without any measuring information. The next step is to use measurements, often noisy measurements, to update the states to a *posteriori* distribution. These steps are recursively performed on each time instant. The equations are similar to equation 2.10 but instead of output $\mathbf{y}_k$, measurements vector $\mathbf{z}_k$ is used (equation 2.11).

$$\begin{aligned} \mathbf{x}_k &= f_{k-1}(\mathbf{x}_{k-1}, \mathbf{u}_{k-1}, \mathbf{v}_{k-1}) \\ \mathbf{z}_k &= h_k(\mathbf{x}_k, \mathbf{u}_k, \mathbf{w}_k) \end{aligned} \tag{2.11}$$

2.4 Kalman filter

The *Kalman filter* is an optimal filter used for smoothing, filtering or prediction (estimation of past, present and future state). It was presented by Rudolph E. Kalman in 1960's [7] and has become widely used ever since.

The approach requires the system to be linear and its distributions to be Gaussian. This makes the filter only applicable to either linear problems or linear approximations of the system. The process equation is then noted as in equation 2.12

$$\mathbf{x}_k = \mathbf{A}\mathbf{x}_{k-1} + \mathbf{B}\mathbf{u}_{k-1} + \mathbf{v}_{k-1} \tag{2.12}$$

And the measurement equation (equation 2.13):

$$\mathbf{z}_k = \mathbf{H}\mathbf{x}_k + \mathbf{w}_k \tag{2.13}$$

The matrices A, B and H are here noted as time-invariant for notation simplicity. The variables $\mathbf{v}$ and $\mathbf{w}$ is uncorrelated white noise normally distributed as in equation 2.14, where Q is the *process noise covariance* and R is *measurement noise covariance*. [12]

$$\begin{aligned} p(v) &\sim N(0, Q) \\ p(w) &\sim N(0, R) \end{aligned} \tag{2.14}$$

2.4.1 Estimation algorithm

Equations 2.12, 2.13 and 2.14 are used to produce the estimation algorithm. The algorithm will produce an *a priori* estimate which will be noted $\hat{x}_k^-$ (scalar representation will be used for simplicity) and a *posterior* estimate noted $\hat{x}_k$. We also introduce *a priori* and *posteriori* estimate errors (equation 2.15) [6].

$$\begin{aligned} \varepsilon_k^- &\equiv x_k - \hat{x}_k^- \\ \varepsilon_k &\equiv x_k - \hat{x}_k \end{aligned} \tag{2.15}$$

The estimation error covariances for the *a priori* and *posteriori* is as in equation 2.16, where $E[\cdot]$ is the expected value function.

$$\begin{aligned} P_k^- &= E[\varepsilon_k^- \varepsilon_k^{-T}] \\ P_k &= E[\varepsilon_k \varepsilon_k^T] \end{aligned} \tag{2.16}$$

Using discrete Kalman filter, the algorithm is split into two steps. The *process update* (sometimes called *time update*) calculates the *a priori* estimation. The *process update* equations (2.17) uses information from previous step together with the process model to try to predict next state.

$$\begin{aligned} \hat{x}_k^- &= A\hat{x}_{k-1} + Bu_{k-1} \\ P_k^- &= AP_{k-1}A^T + Q \end{aligned} \tag{2.17}$$

Second step in discrete Kalman filter is the *measurement update*. This step uses information from measurements to *correct* the predicted estimate from the process update. Introducing the difference between measurements and the predicted state output as the *innovation* $z_k - H\hat{x}_k^-$. The *innovation* is used to update the *posteriori* estimate as in equation 2.18.

$$\hat{x}_k = \hat{x}_k^- + K_k(z_k - H\hat{x}_k^-) \tag{2.18}$$

The term K_k is a "gain" factor on how much information from measurements and prediction that should be used. This gain, called Kalman gain, is calculated to minimize the *posteriori* error covariance. The complete set of equations for the *measurement update* is seen in equation 2.19 [6].

$$\begin{aligned} K_k &= P_k^- H^T (HP_k^- H^T + R)^{-1} \\ \hat{x}_k &= \hat{x}_k^- + K_k(z_k - H\hat{x}_k^-) \\ P_k &= (I - K_k H)P_k^- \end{aligned} \tag{2.19}$$

3 Input data

Input data to the filter algorithm can come from an arbitrary amount of sources. There are a lot of different tire-to-road estimation methods available for this purpose. There are no optimal estimation that fulfills all demands so there are always trade-offs that has to be made. By using several estimation methods we try minimizing the individual weaknesses. Only the estimation methods used in the current filter are evaluated and described further below.

3.1 Stability systems

Maximum possible acceleration is tightly correlated to available friction. Using this knowledge together with several available stability systems gives an opportunity to retrieve a friction estimate. There are several stability systems in the vehicle that utilizes and provides input when they are active. The result from this estimation is an estimate with quite good confidence; the downside is they only provide information when maximum excitation is reached. Since they also lack information about the friction between interventions they are not continuous.

3.1.1 Anti-lock braking system (ABS) estimation

The ABS control system tries to maximize braking ability by controlling slip-ratio. Using this information and listening for ABS actions gives information whether maximum friction is used. This information and an estimate on tire forces produce a friction estimate with good accuracy [3].

3.1.2 Dynamic stability & traction control (DSTC) estimation

This is similar to the ABS estimation describe above. The traction control system tries to optimize traction and thereby acceleration ability to meet the drivers desire. By measuring slip ratio and braking individual wheels to eliminate wheel spin a maximum acceleration is obtained. Listening for this action in the same way as ABS, a quite good estimate is retrieved.

Whenever the vehicle exceeds available acceleration limitations (due to low friction) when cornering, the control systems tries to maintain control of the vehicle by braking individual wheels to counteract the vehicles desire to under- or oversteer. This signal present the same estimate as above [13].

3.2 Road surface classification sensors

Knowing what type of material and surface is beneath the car gives information regarding available friction. By using different methods to classify surface condition a continuous friction estimate can be calculated. Classifying the surface into predefined discrete steps gives opportunity to define friction distribution for these surfaces.

There are several ways to obtain this surface classification. Using camera data and image analysis algorithms is one way. Other solutions are to use specific devices, e.g. RoadEye [14], that illuminates the surface with light and measuring backscattering for different wavelengths, or some sort of communication with other vehicles or infrastructure. There have been several attempts to estimate the surface from vibration models or other vehicle dynamic sensoring methods [15].

These methods don't give a direct measurement of the friction. They only present which predefined surface that is current. Data is needed to produce a priori distribution from these classifications. Although these methods give a continuous estimate the weakness is their quite wide distributions and correlation in time.

Another disadvantage is that it only provides information about the surface. The friction force is generated in the contact area between the tire and the road and the measurements from road surface classification sensors don't supply any information regarding the tire.

3.2.1 Defined surface classifications

The road surface has an enormous amount of possible states. Present road surface can be seen as a continuous state with numerous amount of influencing parameters. To be able to deal with this situation a discretization of the surface classifications is made. The proposed algorithm uses four discrete road surface classifications. Deciding and dividing into these steps was made assuming available sensors and methods could provide these steps. There are however, when more sophisticated and advanced sensors and methods is available, possibility to change these discrete steps into other solutions. The final discrete steps present in the current algorithm are *ice, snow, wet asphalt & dry asphalt*.

Investigation and evaluation of the discrete road surface types lead to the following assumptions. Due to the contemplated fusion algorithm (described in 2.4) the distribution for each surface class is assumed to be distributed with normal Gaussian distribution. Consulting literature, articles and research done in the tire-to-road friction area a suggestion for how the friction is distributed for each surface class is presented as in table 3.1 and figure 3.1. It should be noted here that it is not in the scope of this thesis to evaluate and verify these distributions. This suggestion is mainly based on a literature study made by The Swedish National Road and Transport Research Institute [1], which has summarized several surveys.

Surface	Mean	Standard deviation
Ice	0.15	0.1
Snow	0.3	0.1
Wet asphalt	0.7	0.1
Dry asphalt	0.9	0.1

Table 3.1: Friction distribution parameters for normal gaussian distribution of each surface classification

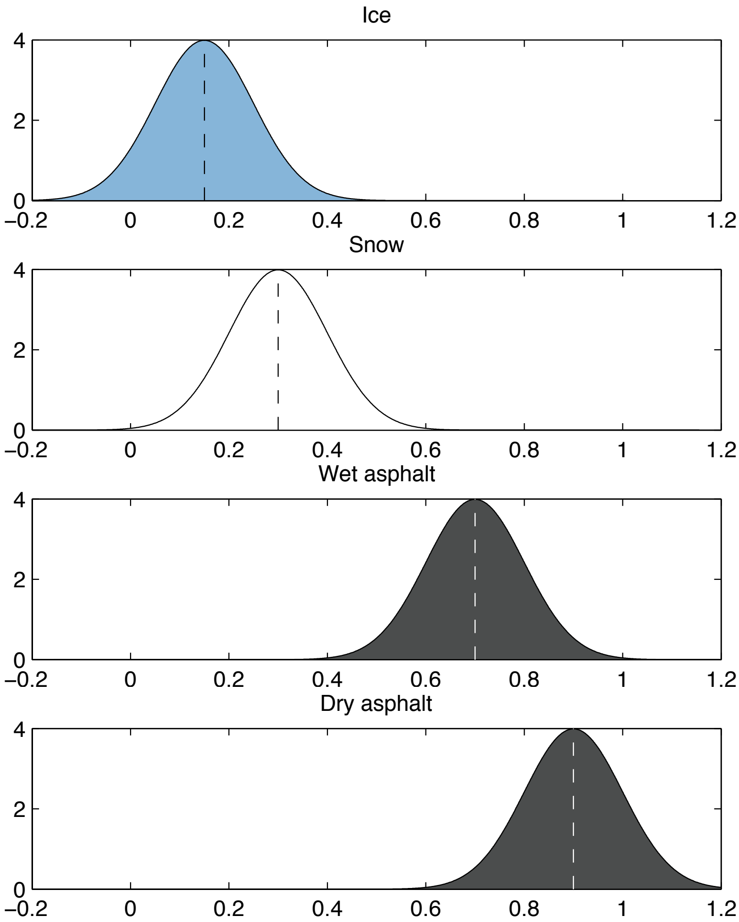

Figure 3.1: *Priori* distributions for ice, snow, wet asphalt and dry asphalt

3.3 Simulating sensor input

The log files that are used in this thesis are recorded without the DSTC and TCS systems. This is to get a good reference speed from the wheels. Because of the need for an estimate from the stability systems in our simulations, all stability systems are simulated. The car is assumed to be all wheel drive to handle the worst case.

To simulate when an intervention would have appeared the normalized acceleration of the longitudinal and lateral acceleration is formed according to the first equation in 3.1. It is then checked when A_{Norm} divided by the gravitational constant g is greater than available friction, see second equation in 3.1.

$$\begin{aligned} A_{Norm} &= \sqrt{A_{Lat}^2 + A_{Long}^2} \\ \frac{A_{Norm}}{g} &> \mu_{available} \end{aligned} \tag{3.1}$$

When the conditions are met it is assumed that an intervention would have appeared and generated a friction estimate. There is also a lower limit on how long time this condition has to be fulfilled in order to generate an estimate. This time is set to 0.5 seconds.

To find out which stability system, i.e. ABS, DSTC or TCS that would have generated the estimate, the angle of the normalized acceleration is used. In table

3.2 the angles for when the different systems is assumed to give information is displayed.

Stability system	Condition for estimate
ABS	$220° < A_{Norm} < 320°$
DSTC	$-50° < A_{Norm} < 50° \vee 130° < A_{Norm} < 230°$
TCS	$40° < A_{Norm} < 140°$

Table 3.2: Conditions for when different stability systems is assumed to generate an estimate

The actual estimate that is generated is assumed to be an unbiased measurement of the current friction; no noise is put on the value. All estimates, i.e. ABS, DSTC and TCS are assumed to have the variance according to section 4.1.

4 Sensor fusion method

This section covers the fusion algorithm and explains why it is chosen. Main focus has been to develop a framework for the data fusion and therefore some assumptions and simplifications have been made. These will be motivated here and possible affects will be discussed in section 8.

Main work of the data fusion is performed in a Kalman filter (theory explained in section 2.4). Maximum available friction μ_{max} is chosen as state variable. The process model (equation 4.1) is chosen as a random walk process[1].

$$\begin{aligned} x_k &= \gamma x_{k-1} + (1-\gamma)\mu + v_{k-1} \\ v_k &\sim N(0, Q) \\ \gamma &\in [0, 1) \end{aligned} \tag{4.1}$$

Using this approach, with parameters γ, μ and Q, makes the *posterior* distribution move toward the proposed *priori* distribution $N(\mu, \tilde{Q})$ when no measurements are available. The convergence using this approach is seen in equation 4.2 [16].

$$\begin{aligned} E[x_{k+l}] &= \gamma^l E[x_k] + \mu(1-\gamma^l) \\ Cov[x_{k+l}] &= \gamma^{2l} Cov[x_k] + \frac{1-\gamma^{2l}}{1-\gamma^2} Q \end{aligned} \tag{4.2}$$

Using values for mean (μ) and covariance ($\tilde{Q}$) from section 3.2.1, with μ as mean and $Q = \tilde{Q}(1-\gamma^2)$ will make the filter approach the predefined distributions for each surface. The use of parameter γ can be seen as a *forgetting factor* and its implementation is described further in section 4.2.

4.1 Measurements

The measuring equations relate measurements to the estimate. Estimation methods, described in section 3.1, gives direct information about maximum friction and are used as measurements as in equation 4.3.

$$\begin{aligned} z_{k,i} &= x_k + w_{k,i} \\ w_{k,i} &\sim N(0, R_i) \end{aligned} \tag{4.3}$$

Measurement error covariance R_i for the ABS estimate is obtained by calculating data variances from a log file of a 2.5 hour long drive in winter conditions. The variance from each intervention is calculated and the mean is formed. The specific drive log contained 60 ABS interventions and the average variance was 0.0033. It is assumed that there is no bias between the measurement and the actual friction coefficient. The error covariance does besides sensor noise also include possible short term friction fluctuations.

The covariances for TCS and DSTC estimates are assumed to be the same as for the ABS estimate. The values are fixed and thus assumed not to depend on velocity.

[1]Note: Unfortunately common notation for both mean (as in statistics) and friction is μ. This might in some equations be confusing. To make it clearer all notations concerning friction will be used with an index, i.e. μ_{max} or $\mu_{available}$.

4.2 Forgetting function

The γ variable is a design parameter. It can be seen as a forgetting factor, and determines convergence speed toward the predefined priori distribution. Our choice is to define a driving distance when the filter only should use 10% of current estimate and 90% of priori distribution. This can be compared to rise time or in this case rise length. Since the filter is run on specified sampling rate, rather than triggered on driven distance, the value needs to be recalculated each iteration with current speed (equation 4.4). T_s is the sampling interval, V_{fwd} is forward velocity and $\lambda_{distance}$ determines the length.

$$\gamma = 0.1^{\frac{|V_{fwd}|T_s}{\lambda_{distance}}} \tag{4.4}$$

4.3 Road surface input

Equation 4.1 uses, besides γ described above, μ and Q. These parameters are specific for each surface and the road surface input then decides which parameters to use (see section 3.2.1).

In order to not lose valuable information gained for a specific surface when switching between surfaces, each defined surface is allocated its own filter. These filters are each run in parallel. Each filter does *process updates* each iteration but only the active filter does *measurement update*. Present version of the fusion filter thus uses four parallel filters $\hat{x}_{k,Ice}$, $\hat{x}_{k,Snow}$, $\hat{x}_{k,WetAsphalt}$ and $\hat{x}_{k,DryAsphalt}$.

5 Performance and functionality

In order to verify performance and functionality of the filter and framework algorithm some tests has been run. Performance measurements are defined in section 5.1 and the scenarios tested are described in 5.2.

5.1 Correctness & Availability

Evaluation of simulation result is done in several ways. The first is to calculate RMS (Root Mean Square) of the error (ε_k) as defined in equation 5.1. The difference between the estimate and the reference is summarized and divided according to equation 5.1, where n is the number of samples.

$$\begin{aligned} \varepsilon_k &= \mu_{ref,k} - \hat{x}_k \\ \varepsilon_{RMS} &= \sqrt{\frac{\sum_{i=1}^{n} \varepsilon_i^2}{n}} \end{aligned} \tag{5.1}$$

High friction values generate less data input than low friction values. This is because the excitation needed to get input is seldom reached in high friction areas. High friction is also considered less dangerous and thus it is not as important to be accurate in high friction as in low. This might make the RMS error value a bit unfair, and thus a proposed *weighted* RMS error value is also used. This value uses ($\varepsilon_{k,weighted}$) instead, se equation 5.2. Since $\mu_{ref,k} \in [0, 1.1]$ lower friction values will affect the RMS more.

$$\varepsilon_{k,weighted} = \frac{\mu_{ref,k} - \hat{x}_k}{\mu_{ref,k}} \tag{5.2}$$

Another interesting aspect is during how long time the estimation and its distribution is within a specified interval. These tests are set up as in equation 5.3. The first equation calculates the ratio of when the estimation error is within $\pm$ 0.1 and the second when the estimate $\pm$ error covariance is within $\pm$ 0.1. When both estimate and actual friction is above 0.5 the estimate is also considered as available and it is therefore included in the equations [17].

$$\begin{aligned} \eta_{\varepsilon\pm0.1} &= \frac{\sum_{i=1}^{n}\{(|\varepsilon_k| \leq 0.1) \vee (\hat{x}_k \geq 0.5 \wedge \mu_{ref,k} \geq 0.5)\}}{n} \\ \eta_{|\varepsilon\pm\sigma|\pm0.1} &= \frac{\sum_{i=1}^{n}\{(|\varepsilon_k \pm \sqrt{P_k}| \leq 0.1) \vee (\hat{x}_k - \sqrt{P_k} \geq 0.5 \wedge \mu_{ref,k} \geq 0.5)\}}{n} \end{aligned} \tag{5.3}$$

5.2 Scenarios

Since simulation model and logged model differ there has to be different scenarios for each model. The Scenario that is run in the simulation model is used to make performance tests and tune parameters. In simulation environment the defined friction profile is used as reference. When running tests on logged data no friction reference is present, and therefore performance tests is harder to evaluate. Important aspects on both scenarios are how the estimate is affected with or without road surface information.

5.2.1 Simulation scenario

Two scenarios has been tested, one with pure simulated inputs and one with logged data. The simulation scenario is chosen with a friction profile as in figure 5.1. The road surface profile is first two sections of snow (with $\mu_{max} = 0.25$ and 0.35), one section ice ($\mu_{max} = 0.10$) followed by one section wet asphalt ($\mu_{max} = 0.8$) and last one section ice again. Each section is 300 seconds long and that makes the complete run 25 minutes. The friction profile is intentionally set with an offset from the predefined *priori* distributions to test the algorithm behavior.

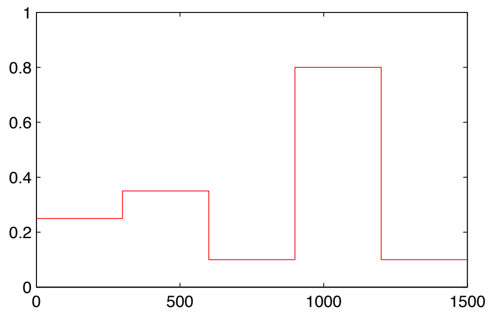

Figure 5.1: Friction reference profile for simulation scenario

The steps changes in the friction profile are to simulate a change in the road surface. The first step change is from one snow to another snow condition. This can for instance be the case when driving on a less traveled road whit loose snow and then reaching a more frequently travelled road which has packed snow.

The remaining three step changes are due to change in road condition that is assumed to be detectable. From snow to ice, then wet asphalt and finally ice again. This can be the case if one enters a road which has been ploughed and where water has frozen on the road surface. Another road segment might be salted, and then it is possible that this section is not frozen even though it has the same temperature.

This simulation scenario is made to stress the filter with step changes which is interesting in a performance testing point of view.

5.2.2 Log scenario

The log scenario is a 5 minutes long run on rural roads in winter conditions. The main road surface is homogenous snow but there are a few shorter ice segments. The speed is about 50-70km/h and it is normal calm driving with almost no other traffic around. Two test breaks are made on the snow in this log and each friction estimate, together with the mean, can be seen in table 5.1.

Because of the homogeneity of the snow and the similarities in the ABS estimates the friction for snow in this scenario is assumed to be the mean of the two. For the

	First ABS	Second ABS	Mean ABS
Estimate	0.286	0.328	0.307

Table 5.1: Test breaks during log: first, second and average of the two

ice there is no information available and it is assumed to have a friction coefficient of 0.15 according to the predefined *priori*.

6 Results - Simulation model

A few tests have been made and the results is categorized as with and without road surface classification. One test with only road surface classification and no direct measurements have also been made as a reference.

Section 5.2 describes set up, methods and assumptions used to run and test the algorithm when using simulated data model.

6.1 Simulation with road surface classification

With observations at ABS/TCS/DSTC interventions the filter has some information, besides the road surface classification, that is used to improve its estimate. At lower friction the excitation rate is higher and thus more information is retrieved. With the friction unit step at 300s without RSC change, the filter does not adapt to the new condition (figure 6.1). In the high friction area ($900s < t < 1200s$ in figure 6.1) no observation is available and the RSC information is the only input.

Correctness and availability measurements (as defined in section 5.1) are seen in table 6.1. The estimation is at all time within reference friction plus/minus 0.1. However, since the estimate is quite unsure at some times the other availability measurement is not as high.

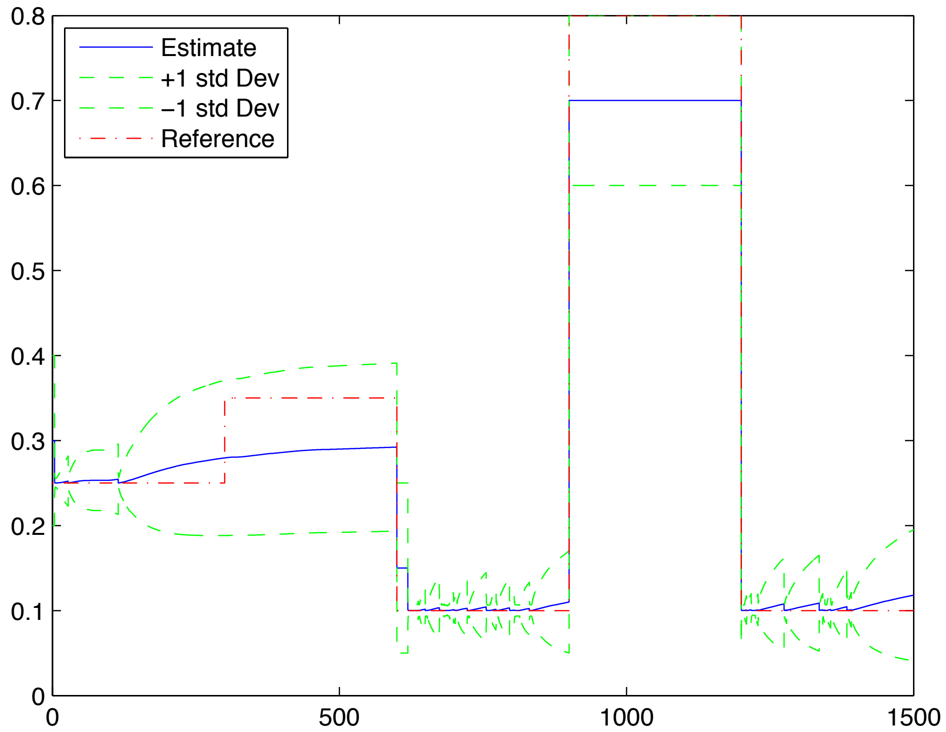

Figure 6.1: Simulation with road surface information and measurements at 100% tire-force utilization

ε_{RMS}	0.0537
$\varepsilon_{RMS,weighted}$	0.1217
$\eta_{\varepsilon\pm0.1}$	1.0000
$\eta_{\lvert\varepsilon\pm\sigma\rvert\pm0.1}$	0.7295

Table 6.1: Simulated result for simulation model with road surface information measurements available at 100% tire-force utilization, tests as defined in section 5.1

6.2 Simulation without road surface classification

These tests are run without information about road surface. The friction profile and tests are the same as mentioned in section 6.1. When no RSC is present, the filter will assume wet asphalt. This makes the algorithm conservative when no direct measurements are available.

Because of the lack of information concerning road surface the estimate drifts towards the *priori* of wet asphalt and produces a fluctuating estimate. In the high friction area ($900s < t < 1200s$ in figure 6.2) no observation is available and the filter does not have enough time to settle during this section. The irregularities seen in the estimate at approximately 300s and 1100s is because of the speed dependence.

In table 6.2 the correctness and availability measurements are presented as defined in section 5.1.

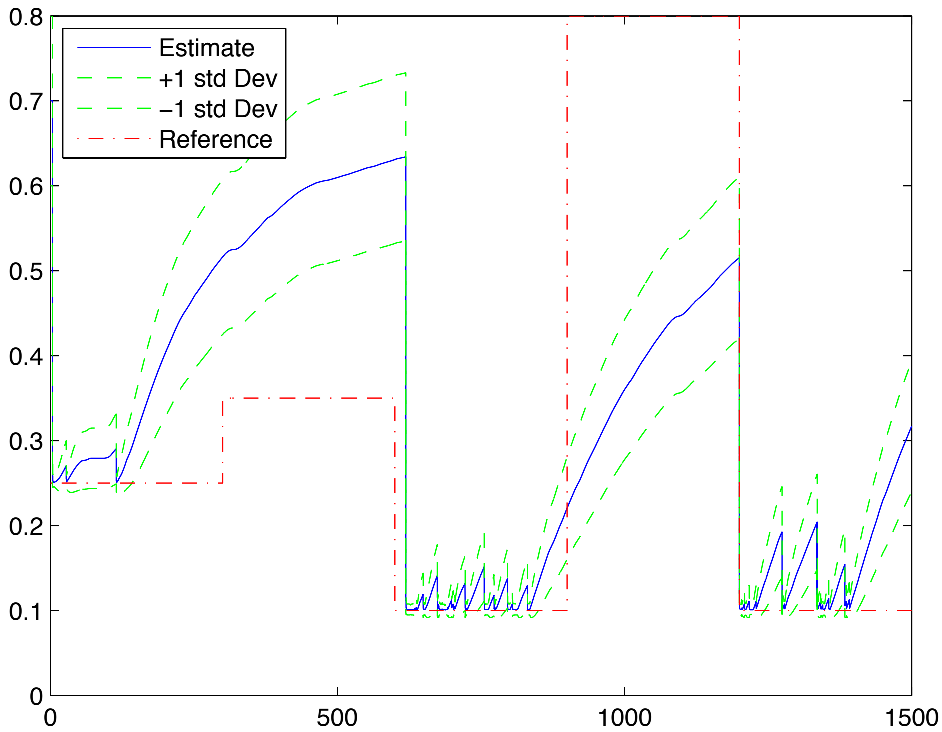

Figure 6.2: Simulation without road surface information and measurements at 100% tire-force utilization

ε_{RMS}	0.2349
$\varepsilon_{RMS,weighted}$	0.8684
$\eta_{\varepsilon\pm0.1}$	0.4621
$\eta_{\vert\varepsilon\pm\sigma\vert\pm0.1}$	0.3716

Table 6.2: Simulated result for simulation model without road surface information measurements available at 100% tire-force utilization, tests as defined in section 5.1

6.3 Simulation with only road surface classification

This test is run with road surface classification and no direct measurements. As can be seen in figure 6.3 the estimate is biased to the reference during the entire run as described in section 5.2.1. The results are mostly of interest if compared to the other runs, see table 6.4

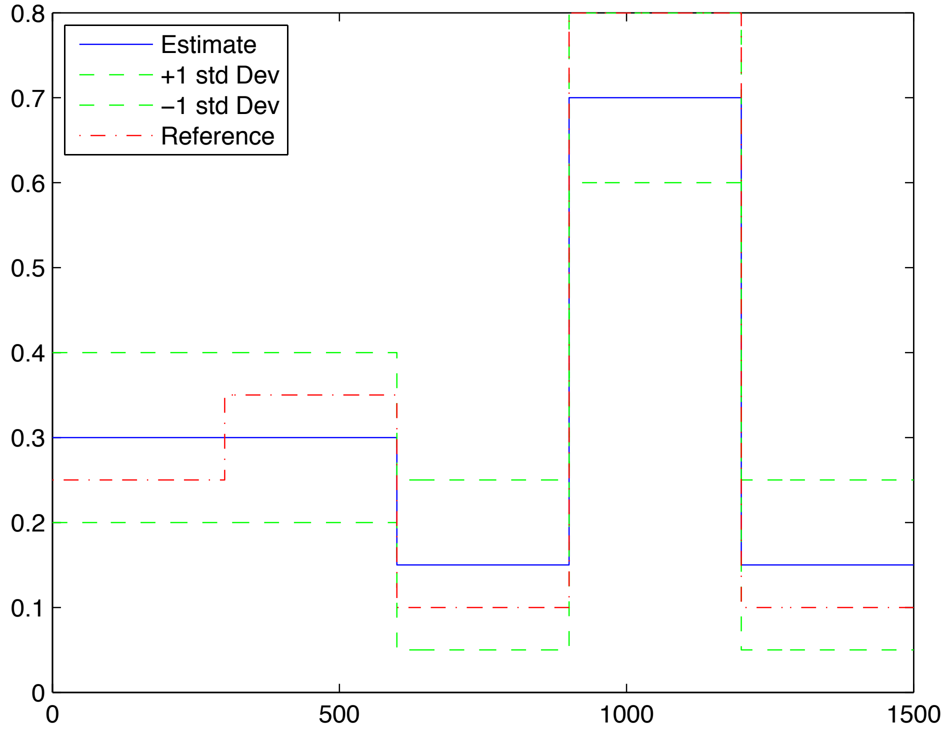

Figure 6.3: Simulation with only road surface information and no other measurements

ε_{RMS}	0.0632
$\varepsilon_{RMS,weighted}$	0.3394
$\eta_{\varepsilon\pm0.1}$	1.0000
$\eta_{\lvert\varepsilon\pm\sigma\rvert\pm0.1}$	0.2000

Table 6.3: Simulated result for simulation model with only road surface information and no other measurements, tests as defined in section 5.1

6.4 Summarized result for simulation model

Values from sections 6.1, 6.2 and 6.3 are summarized in table 6.4. Large differences can be seen when comparing with and without RSC. It can also be noted that fairly good results is shown even if only relying on the road surface classification.

	RSC	No RSC	Only RSC
ε_{RMS}	0.0537	0.2349	0.0632
$\varepsilon_{RMS,weighted}$	0.1217	0.8684	0.3394
$\eta_{\varepsilon\pm0.1}$	1.0000	0.4621	1.0000
$\eta_{\lvert\varepsilon\pm\sigma\rvert\pm0.1}$	0.7295	0.3716	0.2000

Table 6.4: Summarized simulation result, tests as defined in section 5.1

7 Results - LoggData model

A few simulation tests are run with data recorded from a logged run. The log is from a five minute long run during winter conditions with homogenous snow and spots of ice.

When using logged data no friction reference is present. Examination of brake tests done in the runs is used to make an assumption of possible friction reference. Investigation of recorded video sequence from the same occasion is made to increase the confidence. Using reference in these tests does not ensure an absolute result, but can be used to note and estimate tendencies or investigate a specific scenario.

7.1 Simulation with road surface classification

The data logs are recorded with data from a Road-Eye sensor (described in section 3.2). This sensor has recorded backscattering and an algorithm classifies the road surface with a neural network approach. Visual investigation of recorded video sequence from the logged run is made to validate its correctness.

Full force-utilization uses ABS/TCS/DSTC interventions as input data to the filter. Since the recorded run is made with TCS and DTCS shut off, these signals are recreated in the simulation. No interventions at all where present during the run and the algorithm relies completely on its *a priori* as seen in figure 7.1. Table 7.1 notes the performance of the algorithm for the specified sequence.

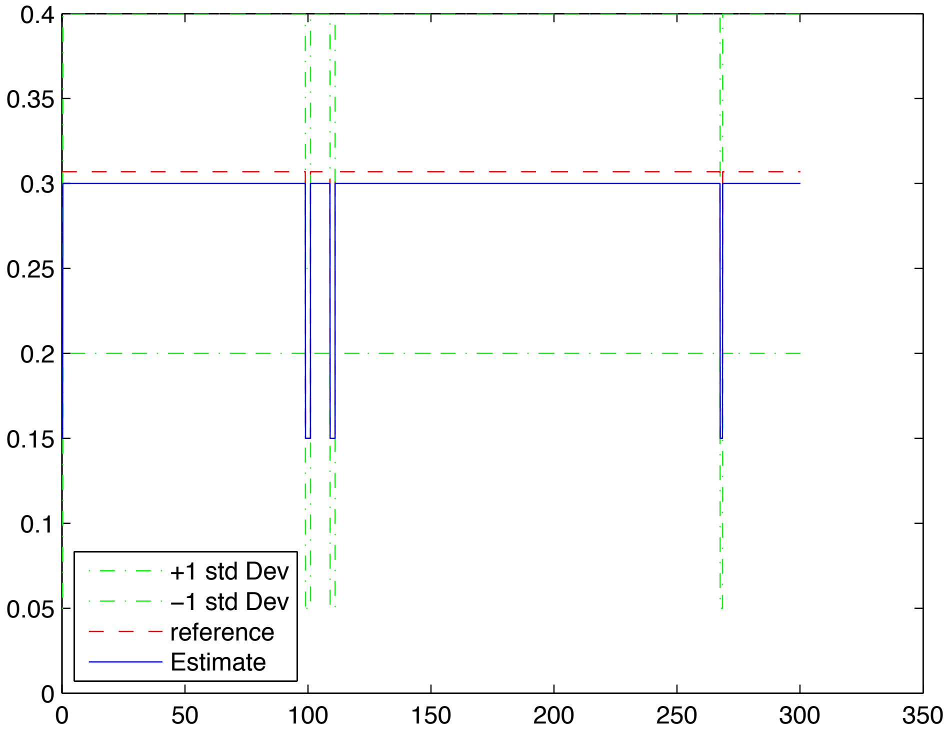

Figure 7.1: Logged data simulation with road surface information and measurements at 100% tire-force utilization

ε_{RMS}	0.0087
$\varepsilon_{RMS,weighted}$	0.0285
$\eta_{\varepsilon \pm 0.1}$	0.9988
$\eta_{\|\varepsilon \pm \sigma\| \pm 0.1}$	0.0000

Table 7.1: Simulated result for logged data model with road surface information measurements available at 100% tire-force utilization, tests as defined in section 5.1

7.2 Simulation without road surface classification

Tests without the road surface information are run in the same way as noted in section 7.1. Just as in section 7.1 no interventions is present during the simulation. Without RSC in this simulation the estimation has no information which results in large errors (figure 7.2) and poor performance (table 7.2).

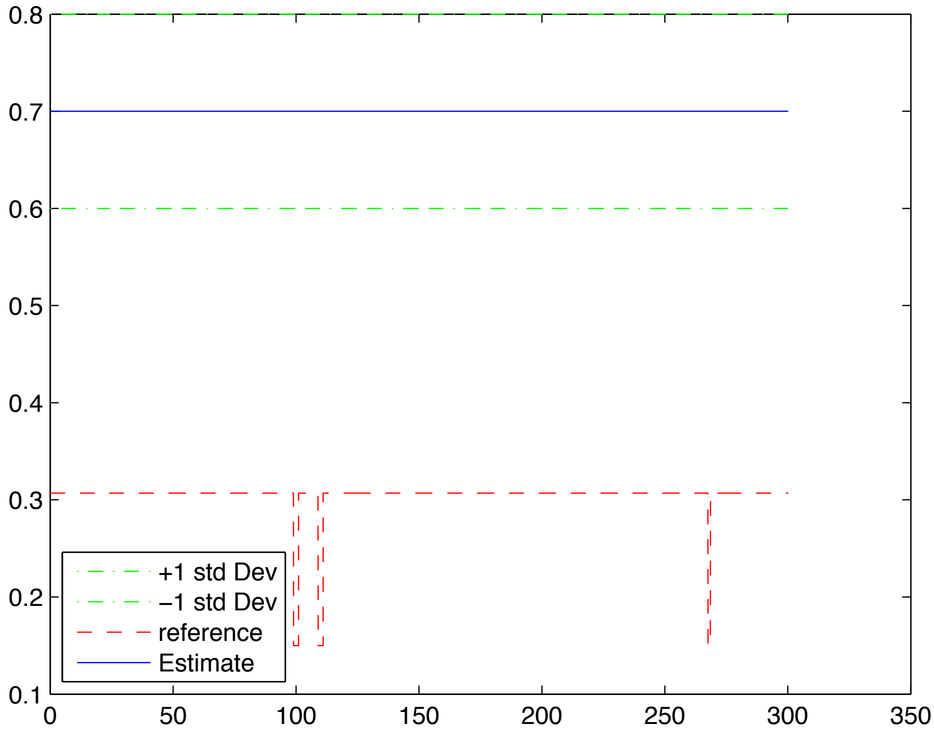

Figure 7.2: Logged data simulation without road surface information and measurements at 100% tire-force utilization

ε_{RMS}	0.3962
$\varepsilon_{RMS,weighted}$	1.3571
$\eta_{\varepsilon\pm0.1}$	0.0000
$\eta_{\lvert\varepsilon\pm\sigma\rvert\pm0.1}$	0.0000

Table 7.2: Simulated result for logged data model without road surface information measurements available at 100% tire-force utilization, tests as defined in section 5.1

7.3 Summarized result for loggdata model

Values from sections 7.1 and 7.2 are summarized in table 7.3. The difference between having a road surface classification and not having one is shown in most performance measurements.

	RSC	No RSC
ε_{RMS}	0.0087	0.3962
$\varepsilon_{RMS,weighted}$	0.0285	1.3571
$\eta_{\varepsilon\pm0.1}$	0.9988	0.0000
$\eta_{\lvert\varepsilon\pm\sigma\rvert\pm0.1}$	0.0000	0.0000

Table 7.3: Summarized simulation result from logged data, tests as defined in section 5.1

8 Discussion

One of the problems in this project has been the absence of a good reference on the friction coefficient. By simulating estimations from stability systems based on acceleration measurements, and a predefined friction profile, this has in some sense been circumvented. This simulation comes with some assumptions.

The log data is gathered in winter conditions under rural road driving and it's assumed that the driving behavior is representative for all road conditions in the friction profile. This assumption might be a bit conservative for the high friction areas on which maybe a more aggressive driving behavior normally is used.

The assumption that the stability systems give an unbiased estimate might be optimistic. There is also the possibility that the DSTC estimates do not have the same variance, which is assumed in this report.

Using a normal Kalman filter restricts the filter to only handling normal distributions. This means that the uncertainty is equally large over and under the estimate. This restricts the behavior that is possible to achieve and causes some properties that might be unwanted.

The a priori for the different road surface classifications might not be sufficiently approximated with a normal distribution. It might be possible to get a better result if the output is allowed to have a different distribution. The variance of the measurements is probably well approximated with normally distributed noise, this assuming that they are unbiased.

Result discussion The RMS error value ε_{RMS} is a bit rough because the measurement is heavily increased in the high friction area where no direct estimates are available. The weighted RMS error $\varepsilon_{RMS,weighted}$ presents a more interesting measurement of the relation between the different tests. A big difference is seen if a RSC is available or not. This is mainly due to two things, first the high friction area, where the test with RSC detects the change directly and makes a step change to the *a priori* for the new road surface. The second thing that keeps the RMS value small is the fact that the *a priori* and the estimate are never largely biased when a RSC is available. The forgetting factor is set on forgetting 90% of the bias over a specified distance. If the bias is small the estimate does not drift as much with distance as if the bias is large.

The availability measurement $\eta_{\varepsilon\pm0.1}$ only takes the estimate into account and does not depend on the distribution. This makes it possible to acquire full availability in the tests with RSC even if the estimate is unsure. This is especially obvious in the comparison test where only RSC is used. A more interesting measurement is the availability measurement $\eta_{|\varepsilon\pm\sigma|\pm0.1}$ that also depends on the certainty in the distribution. Two notable results can be seen in table 6.4, first the fact that the run with RSC has about twice as good availability as the test without RSC. Secondary it can be seen that only RSC does not generate good $\eta_{|\varepsilon\pm\sigma|\pm0.1}$ availability if no other measurements are available.

9 Conclusions

The proposed fusion algorithm, works as intended and is able to combine both direct and indirect measurement inputs. It shows good potential for tire-to-road friction estimation problems. The approximated linear process model makes the filter handle model uncertainties and short term fluctuations well. Even with less available tire-to-road friction information the filter produce good result with small estimation error.

A road surface classification shows good potential of improving both availability and correctness of the friction estimate. The response time after a surface change can be greatly reduced. The estimate drifts with a slower speed due to the *a priori* having a small bias to the true friction value.

The road surface classification greatly reduces the RMS error due to its short ramp up time when changing road surface to wet or dry asphalt. The RSC also enables the filter to keep information about a former road surface even if new information is gathered about the present road surface.

10 Future work

In this section some suggestions on further development is proposed.

Utilized acceleration Accelerometers give constant information about utilized acceleration. This measurement give information on what μ_{max} isn't. This information can be used to correct the friction estimate when μ_{max} is underestimated. Letting the acceleration measurement truncate the distribution of the estimate, and then recalculating a new Gaussian distribution, and use this to update the estimate can enhance the result.

***A priori* distributions** The distributions for friction on different surfaces can be further investigated. For example thorough test can be made with different cars and tires on the different surfaces to get a better picture of the PDF. These tests can also reveal if the assumption of normally distributed PDF is a good approximation. It is preferable if the tests can be made on the specific surfaces that are detectable with sensors.

Statistical approach to simulating input data By investigating recorded data logs driven on a specific road surface the frequency and also PDF of 100% utilized friction can be found. It can then be used to generate input data to the estimation algorithm based on road surface. In this way the driver behavior for a specific road condition is included in the simulation. Another approach is to map the change in velocity and used acceleration on different road surfaces.

More advanced and flexible simulations If a more advanced simulation environment is used some of the assumptions made in this thesis can be validated and sometimes avoided. By using a more advanced simulation tool, driver behavior can be modified depending on several parameters. Some investigations for instance claim a change in driving behavior due to the visible change in weather and road surface condition [1]. The stability systems can be simulated and the friction estimate generated from them can be more realistically created.

Handling uncertainties in the RSC To have a robust algorithm that works with real input data from a RSC information source the algorithm has to cope with uncertainties of some sort. One way of doing this is to use interacting multiple model (IMM). This model forms an optimal weighted sum of the output from the filters of each road surface.

References

[1] C.-G. Wallman and H. Åström, "Friction measurement methods and correlation between road friction and traffic safety.," *VTI meddelande*, no. 911A, 2001.

[2] R. Rajamani, *Lateral and Longitudinal tire forces.* Springer, 2006.

[3] D. Capra, N. D'Alfio, A. Morgando, and A. Vigliani, *Experimental Test of Vehicle Longitudinal Velocity and Road Friction Estimation for ABS System.* SAE International, 2009.

[4] J. Svendenius, *Tire Modeling and Friction Estimation.* PhD thesis, Department of Automatic Control, Lund University, 2007.

[5] B. Mulgrew, P. Grant, and J. Thompson, *Digital Signal Processing - Concepts and Applications.* Palgrave McMillan, 2 ed., 2003.

[6] G. Welch and G. Bishop, "An Introduction to the Kalman Filter," *Department of Computer Science, University of North Carolina*, 2006.

[7] R. E. Kalman, "A New Approach to Linear Filtering and Prediction Problems," *Research Institute for Advanced Study*, 1960.

[8] B. Ristic, S. Arulampalam, and N. Gordon, *Beyond the Kalman Filter, Particle filters for tracking applications.* Artech House Publishers, 2004.

[9] K. J. Åström and B. Wittenmark, *Computer Controlled Systems, Theory and Design.* Prentice Hall, Inc., 1997.

[10] R. Serfozo, *Basics of Applied Stochastic Processes.* Springer, 2009.

[11] T. Glad and L. Ljung, *Control Theory, Multivariable and Nonlinear Methods.* Taylor & Francis, 2000.

[12] S. Haykin, *Kalman Filtering and Neural Networks.* John Wiley & Sons, Inc., 2001.

[13] S. Koskinen, *Sensor Data Fusion Based Estimation of Tyre-Road Friction to Enhance Collision Avoidance.* PhD thesis, Tampere University of Technology, 2010.

[14] J. Casselgren, *Road surface classification using near infrared spectroscopy.* PhD thesis, Luleå University of Technology, 2007.

[15] T. Umeno, E. Ono, and K. Asano, "Estimation of Tire-Road Friction Using Tire Vibration Model," in *Vehicle Dynamics and Simulation*, 2002.

[16] J. Sörstedt, L. Svensson, F. Sandblom, and L. Danielsson, "A new vehicle motion model for improved predictions and situation assessment," 2007.

[17] P. Westergren, "VVTBT Bitumenbindna lager 09," *Vägverket 2009:140*, 2009.